IEEE Access
Multidisciplinary ⋮ Rapid Review ⋮ Open Access Journal

Received 27 November 2023, accepted 3 December 2023, date of publication 12 December 2023, date of current version 20 December 2023.

Digital Object Identifier 10.1109/ACCESS.2023.3341425

RESEARCH ARTICLE

Finite-Horizon Variance-Constrained H_∞ Estimation for Complex Networks Subject to Dynamical Bias Using Binary Encoding Schemes

WEIJIAN LI[1,2,3,4], NAN HOU[1,2,3,4], FAN YANG[1,2,3,4], XIANYE BU[1,2,4,5], AND LIGANG SUN[6]
[1]National Key Laboratory of Continental Shale Oil, Northeast Petroleum University, Daqing 163318, China
[2]Sanya Offshore Oil & Gas Research Institute, Northeast Petroleum University, Sanya 572025, China
[3]Artificial Intelligence Energy Research Institute, Northeast Petroleum University, Daqing 163318, China
[4]Heilongjiang Provincial Key Laboratory of Networking and Intelligent Control, Northeast Petroleum University, Daqing 163318, China
[5]School of Electrical & Information Engineering, Northeast Petroleum University, Daqing 163318, China
[6]CenerTech Tianjin Chemical Research and Design Institute Company Ltd., Tianjin 300131, China

Corresponding author: Xianye Bu (xianyebu@gmail.com)

This work was supported in part by the Hainan Provincial Joint Project of Sanya Yazhou Bay Science and Technology City of China under Grant 2021JJLH0025; in part by the Hainan Province Science and Technology Special Fund of China under Grant ZDYF2022SHFZ105; in part by the National Natural Science Foundation of China under Grant U21A2019, Grant 62203105, Grant 62103096, and Grant 62073070; in part by the Natural Science Foundation of Heilongjiang Province of China under Grant YQ2023F003; and in part by the Fundamental Research Funds for Undergraduate Universities Affiliated to Heilongjiang Province of China under Grant 2022TSTD-04.

ABSTRACT In this article, a variance-constrained H_∞ state estimation issue is dealt with for a type of nonlinear time-varying complex networks affected by dynamical bias under binary encoding schemes (BESs). The BESs are used during signal transmission in view of the security of binary bit strings. The stochastic bias is involved using a dynamical equation, and stochastic nonlinearity is characterized by statistical property. The purpose of this article is to construct a finite-horizon state estimator, such that the estimation error dynamics satisfies performance requirements of both the prescribed upper bound constraint on the error variance and the H_∞ noise rejection. By employing the matrix inequality approach and random analysis, sufficient conditions are established for the presence of the state estimator. Subsequently, the gain parameters of the constructed estimator are acquired by solving some recursive matrix inequalities. Ultimately, the correctness of the developed estimation algorithm is testified via a numerical simulation example.

INDEX TERMS Time-varying complex networks, binary encoding schemes, variance-constrained state estimation, dynamical bias, stochastic nonlinearities.

I. INTRODUCTION

As we all know, the complex networks (CNs) consist of numerous nodes, which are coupled with each other. Therefore, it is necessary to think over both the dynamics of each node and the coupling configuration between them in the analysis of CNs [1], [2], [3], [4], [5], [6]. CNs include all kinds of natural or artificial networks, such as computer networks, gene networks, transportation networks, biological networks, and social networks. Due to the successful application of CNs in a variety of real-world systems, they have attracted high investigation attention with numerous valuable results [7]. Up to now, a substantial number of literature has been concerned with the dynamic analysis of CNs [8]. Among the current research results, the state estimation (SE) issues have received significant attention due to that the network state cannot usually be measured directly from the network output, especially for large-scale networks [9], [10], [11], [12], [13], [14]. For instance, the SE issue has been studied in [9] for a type of random CNs with encoding-decoding strategies and stochastic coupling parameters. On the basis of the Round-Robin protocol, the H_∞ SE problem has been tackled in [10] for a kind of nonlinear singularly perturbed CNs. The effect of the coupling parameter has been fully

The associate editor coordinating the review of this manuscript and approving it for publication was Pinjia Zhang.

considered in [12] on the SE performance, where the topology has been described by a series of time-varying parameters. A zonotopes-based method has been proposed and used in [13] to address the set-membership SE issue for a type of CNs based on the event-triggered scheme.

In the engineering-oriented SE problems, it is very common for upper bound constraint on the error variance to be used to express performance requirements [15], [16], [17], [18]. The variance-constrained SE aims to construct the state estimator within the acceptance range of estimation error, to be specific, it ensures that the variance of the estimation error meets a predetermined upper bound constraint. In comparison with the optimal estimation under the constraint of the minimum error variance, the variance-constrained SE is more flexible and closer to the reality due to that it no longer seeks optimality (i.e., minimum variance). Variance-constrained SE is able to not only impose an upper bound on the error variance, but also leave space for realizing other performance indices due to the flexibility of its design [19]. Accordingly, the problem of variance-constrained state estimator design has attracted a great deal of research interest [17], [20], [21], [22], [23]. More specifically, in [22], the multiobjective (i.e., variance-constrained H_∞) control issue has been considered for discrete time-varying systems with stochastic nonlinearity. The variance-constrained SE issue has been investigated in [21] for a kind of networked multi-rate systems, and sensor failures have been considered that are caused by network issues and measurement quantization. Recently, a variance-constrained fusion estimator has been constructed in [23] for cyber-physical systems to alleviate the negative effect caused by system nonlinearity, stochastic communication protocol scheduling, and denial-of-service attacks. In view of the available literature, the problem of variance-constrained SE for nonlinear time-varying CNs, despite its practical relevance, has not been studied adequately and still needs more attention.

In practice, engineering systems are commonly subject to different types of disturbances caused possibly by unmodeled dynamics or external excitations, which should be properly handled [11], [24], [25], [26], [27], [28], [29]. Stochastic bias is considered as a special kind of unknown disturbance under which the modeling and analysis of the system becomes more difficult and complex. Therefore, significant emphasis has been placed on resolving the simultaneous estimation issue of system state and dynamic bias. For example, the SE issues have been tackled in [30] and [31] subject to stochastic bias. The stochastic bias has been characterized by a dynamical equation as a special type of unknown input, which has been handled via utilizing the augmentation method. In [32], a distributed recursive filter has been designed for a specific type of sensor network that is affected by stochastic bias and packet disorders. Nevertheless, up to now, the estimation problem for CNs with stochastic bias has not gained enough attention, which inspires the work of this paper.

Compared with analog signals, using digital signals in data transmission has the advantages of strong anti-interference ability, high communication reliability, resource-saving, long transmission distance, and easy encryption [33], [34], [35], [36], [37], [38], [39]. As the typical digital signal transmission strategy, the binary encoding schemes (BESs) have been widely used for their unique advantages in improving communication efficiency and enhancing the security of data transmission, by which digital data are represented by using symbols 0 and 1 [36], [40], [41], [42]. As a result of the presence of channel noise in the binary symmetric channel (BSC), it is inevitable that bit errors occur during the transmission of binary bit strings (BBSs), i.e., the BBSs may flip randomly with a crossover probability. This situation would cause the output signal of the decoder to have some deviations from the original measurement output of the sensor, and then the estimation performance may decrease inevitably. Therefore, how to mitigate the impact of bit errors is the key to guaranteeing the estimation performance. In recent years, there has been an increasing focus on studying the influence of random bit errors on estimation performance [43], [44], [45]. However, the BESs related topic has not been studied further yet such as variance-constrained SE for CNs, which requires more attention.

Motivated by the preceding discussion, this article aims to investigate variance-constrained H_∞ state estimation issue for a type of time-varying CNs with dynamical bias and stochastic nonlinearities under the BESs. The major challenges to be tackled are that: 1) how to solve the effect of random bit error on the design of the state estimator for complex networks? and 2) how to derive the state estimator such that, under the BESs, the estimation error dynamics fulfills the performance requirements of both the prescribed upper bound constraint on the error variance and the H_∞ noise rejection? *Highlights of this article are emphasized as below: 1) the system under study is more comprehensive and closer to practical cases, which includes random bias, stochastic nonlinearity, and time-varying parameters; 2) the finite-horizon variance-constrained H_∞ SE issue is firstly addressed concerning nonlinear stochastic CNs under BESs; and 3) the estimator gains are acquired through computing a group of recursive matrix inequalities (RMIs), which is thus suitable for real-time operation.*

The remainder content of this paper is arranged in the following parts. In Section II, mathematical models of complex network and estimator, the problem to be tackled and performance requirements have been presented. In Section III, the variance-constrained H_∞ performance analysis and estimator design have been carried on. In Section IV, a simulation example has been conducted to testify the correctness of the developed variance-constrained H_∞ estimation method. In Section V, conclusions have been summarized about the work of this paper.

Notation: The notation used in this article is fairly standard. $\|\cdot\|$ denotes the standard norm symbol. $\mathbb{R}^n$ is the space of

n-dimensional Euclidean space. For a matrix B, B^{-1}, B^T, tr$\{B\}$ and $B > 0$ ($B \geq 0$) illustrate, respectively, the inverse of B, the transpose of B, the trace of B and B is positive-definite (positive semi-definite). The symbol $\otimes$ expresses the Kronecker product. $I_{(m)}$ represents the identity matrix with the dimension $m \times m$. $\mathbb{V}\{v\}$ and $\mathbb{E}\{v\}$ denote, respectively, the variance and the expectation of the random variable/vector v. diag$\{\ldots\}$ indicates a block-diagonal matrix. 1_p means $[\underbrace{1\ 1\ \cdots\ 1}_{p}]^T$.

II. PROBLEM FORMULATION AND PRELIMINARIES

A. THE MODEL OF COMPLEX NETWORK

Taking account of a kind of nonlinear time-varying CNs over a time horizon $[0, \mathcal{N}]$:

$$\begin{cases} x_i(\flat+1) = A_i(\flat)x_i(\flat) + \sum_{j=1}^{U} a_{ij}\Gamma x_j(\flat) + B_i(\flat)b_i(\flat) \\ \qquad + E_i(\flat)g(\flat, x_i(\flat)) + F_i(\flat)w_i(\flat) \\ z_i(\flat) = L_i(\flat)x_i(\flat) \quad i = 1, 2, \ldots, U \end{cases} \tag{1}$$

where $x_i(\flat) \in \mathbb{R}^{l_x}$ denotes the system state and $z_i(\flat) \in \mathbb{R}^{l_z}$ denotes the output signal; $g(\flat, x_i(\flat)) \in \mathbb{R}^{l_x}$ is a stochastic nonlinear function; $w_i(\flat) \in \mathbb{R}^{l_w}$ is a bounded random process noise of the ith node, which is a mutually uncorrelated zero-mean sequence with $\mathbb{E}\{w_i(\flat)w_i^T(\flat)\} = w_0^2$ ($w_0 > 0$); $A_i(\flat)$, $B_i(\flat)$, $E_i(\flat)$, $F_i(\flat)$ and $L_i(\flat)$ represent the given system matrices with suitable dimensions; $\Gamma = \text{diag}\{\alpha_1, \alpha_2, \ldots, \alpha_{l_x}\} \geq 0$ is the inner coupling matrix; $\Lambda = [a_{ij}] \in \mathbb{R}^{U \times U}$ is the outer coupling strength matrix. If a connection exists between nodes i and j ($i \neq j$), $a_{ij} > 0$; otherwise, $a_{ij} = 0$. Generally, Λ satisfies $\Lambda = \Lambda^T$ and $\sum_{j=1}^{U} a_{ij} = \sum_{j=1}^{U} a_{ji} = 0$.

$b_i(\flat) \in \mathbb{R}^{l_b}$ is the unknown random bias, whose dynamic model is described as follows:

$$b_i(\flat+1) = G_i(\flat)b_i(\flat) + H_i(\flat)\beta_i(\flat) \tag{2}$$

where $\beta_i(\flat)$ indicates the bounded stochastic noise sequence satisfying $\mathbb{E}\{\beta_i(\flat)\} = 0$ and $\mathbb{V}\{\beta_i(\flat)\} = \beta_0^2$ with $\beta_0 > 0$. $G_i(\flat)$ and $H_i(\flat)$ are known matrices with suitable dimensions.

The stochastic nonlinear function $g(\flat, x_i(\flat)) \in \mathbb{R}^{l_x}$ with the initial condition $g(\flat, 0) = 0$ satisfies:

$$\begin{cases} \mathbb{E}\{g(\flat, x_i(\flat))|x_i(\flat)\} = 0 \\ \mathbb{E}\{g(\flat, x_i(\flat))g^T(j, x_i(j))|x_i(\flat)\} = 0, \flat \neq j \\ \mathbb{E}\{g(\flat, x_i(\flat))g^T(\flat, x_i(\flat))|x_i(\flat)\} \\ \quad = \sum_{r=1}^{q} \pi_r(\flat)\pi_r^T(\flat)\mathbb{E}\{x_i^T(\flat)\Pi_r(\flat)x_i(\flat)\} \\ \quad \triangleq \sum_{r=1}^{q} \Theta_r(\flat)\mathbb{E}\{x_i^T(\flat)\Pi_r(\flat)x_i(\flat)\} \end{cases} \tag{3}$$

where q is a given positive integer, $\pi_r(\flat)$ is a prescribed vector, and $\Theta_r(\flat)$ and $\Pi_r(\flat)(r = 1, 2, \ldots, q)$ are given matrices of suitable sizes.

The expression of the measurement signal is provided as follows:

$$y_i(\flat) = C_i(\flat)x_i(\flat) + D_i(\flat)v_i(\flat) \tag{4}$$

where $y_i(\flat) \in \mathbb{R}^{l_y}$ is the measurement signal of node i ($i = 1, 2, \ldots, U$); $C_i(\flat)$ and $D_i(\flat)$ are given matrices with compatible sizes; and $v_i(\flat) \in \mathbb{R}^{l_v}$ represents the bounded stochastic noise, characterized as a zero-mean random sequence with $\mathbb{E}\{v_i(\flat)v_i^T(\flat)\} = v_0^2$ and v_0 is a positive scalar.

Denoting $\bar{x}_i(\flat) \triangleq [x_i^T(\flat)\ b_i^T(\flat)]^T$ and $\bar{w}_i(\flat) \triangleq [w_i^T(\flat)\ \beta_i^T(\flat)]^T$, according to (1) and (2), the following augmented system can be obtained:

$$\bar{x}_i(\flat+1) = \bar{A}_i(\flat)\bar{x}_i(\flat) + \sum_{j=1}^{U} a_{ij}\bar{\Gamma}\bar{x}_j(\flat) + \bar{E}_i(\flat)g(\flat, I_A\bar{x}_i(\flat)) + \bar{F}_i(\flat)\bar{w}_i(\flat) \tag{5}$$

$$y_i(\flat) = \bar{C}_i(\flat)\bar{x}_i(\flat) + D_i(\flat)v_i(\flat) \tag{6}$$

$$z_i(\flat) = \bar{L}_i(\flat)\bar{x}_i(\flat) \tag{7}$$

where

$$\bar{A}_i(\flat) \triangleq \begin{bmatrix} A_i(\flat) & B_i(\flat) \\ 0 & G_i(\flat) \end{bmatrix}, \ \bar{E}_i(\flat) \triangleq \begin{bmatrix} E_i(\flat) \\ 0 \end{bmatrix},$$
$$I_A \triangleq [I_{(l_x)}\ 0], \ \bar{\Gamma} \triangleq \text{diag}\{\Gamma, 0\}, \ \bar{C}_i(\flat) \triangleq [C_i(\flat)\ 0],$$
$$\bar{F}_i(\flat) \triangleq \text{diag}\{F_i(\flat), H_i(\flat)\}, \ \bar{L}_i(\flat) \triangleq [L_i(\flat)\ 0].$$

B. THE ADOPTION OF BINARY ENCODING SCHEMES

In this article, the BESs are adopted in the transmission of measurement signal ($y_i(\flat)$, $i = 1, 2, \ldots, U$) from the sensor to the state estimator. Assuming the scalar signal $y_i(\flat)$ has a range $[-\sigma, \sigma]$, where $\sigma > 0$. By utilizing the encoder, the signal $y_i(\flat)$ is transformed into a BBS of length M. Consequently, we have 2^M points denoted by

$$\mathcal{P} \triangleq \{\tau_{(1)}, \tau_{(2)}, \ldots, \tau_{(2^M)}\}.$$

These points divide the whole range into $2^M - 1$ segments. Each segment has a uniform interval length $\varrho = \tau_{(\rho+1)} - \tau_{(\rho)}$, for $\rho = 1, 2, \ldots, 2^M - 1$. Additionally, it can be observed that

$$\varrho = \frac{2\sigma}{2^M - 1}. \tag{8}$$

Then, a probabilistic quantizer is utilized to obtain the quantized output signal $\vec{y}_i(\flat)$.

The quantized signals are first encoded by the encoder as BBSs and then transmitted through the BSC. During transmission, the BBSs may flip randomly with a probability p (crossover probability) due to the presence of channel noise. After recovering the received binary strings, the decoder forwards the decoded signal to the estimator.

Lemma 1 ([43]): Represent $\zeta_i(\flat) \triangleq \vec{y}_i(\flat) - y_i(\flat)$ as the quantization error. $\zeta_i(\flat)$ is a stochastic variable satisfying

$$\mathbb{E}\{\zeta_i(\flat)\} = 0, \ \mathbb{V}\{\zeta_i(\flat)\} \triangleq \zeta_0^2 \leq \frac{\varrho^2}{4}.$$

Lemma 2 ([43]): Denote $\breve{y}_i(\flat)$ as the output signal of decoder and $h_i(\flat) \triangleq \breve{y}_i(\flat) - \vec{y}_i(\flat)$ as the equivalent noise reflecting bit error. The stochastic term $h_i(\flat)$ is characterized by the following expectation and variance:

$$\mathbb{E}\{h_i(\flat)\} = 0, \ \mathbb{V}\{h_i(\flat)\} \triangleq h_0^2 = \frac{4p(1-p)(2^{2M}-1)\sigma^2}{3(1-2p)^2(2^M-1)^2}.$$

According to the analyses above, the signal received by the estimator can be represented as follows:

$$\breve{y}_i(\flat) = y_i(\flat) + \zeta_i(\flat) + h_i(\flat) \tag{9}$$

Remark 1: Probabilistic quantization is a stochastic method where the expectation of the quantization error is zero [43]. In this article, the quantization error is a bounded random variable with zero expectation and an upper bound on the variance ($\frac{\varrho^2}{4}$).

Remark 2: Equation (9) expresses the received signal of the estimator using the output signal $y_i(\flat)$, quantization error $\zeta_i(\flat)$, and equivalence noise reflecting bit error $h_i(\flat)$, which greatly facilitates the construction of the estimator.

Remark 3: In this study, the occurrence probability of bit errors (crossover probability) can be regarded as the bit error rate, which is calculated as the ratio of the number of erroneous bits to the total number of transmitted bits. Bit errors can cause measurement deviations, which may lead to a reduction in communication accuracy and quality, and ultimately a degradation in estimation performance.

C. THE MODEL CONSTRUCTION OF STATE ESTIMATOR

By virtue of the decoder output signal $\breve{y}_i(\flat)$, we construct the time-varying estimator with the following model:

$$\begin{cases} \hat{x}_i(\flat+1) = \bar{A}_i(\flat)\hat{x}_i(\flat) + \sum_{j=1}^{U} a_{ij}\bar{\Gamma}\hat{x}_j(\flat) + S_i(\flat) \\ \qquad \times(\breve{y}_i(\flat) - \bar{C}_i(\flat)\hat{x}_i(\flat)) \\ \hat{z}_i(\flat) = \bar{L}_i(\flat)\hat{x}_i(\flat), \ i = 1, 2, \ldots, U \end{cases} \tag{10}$$

where $\hat{x}_i(\flat)$ and $\hat{z}_i(\flat)$ represent the estimates of $\bar{x}_i(\flat)$ and $z_i(\flat)$, respectively. $S_i(\flat)$ $(i = 1, 2, \ldots, U)$ describes the unknown gain parameters to be determined.

Defining $e_i(\flat) \triangleq \bar{x}_i(\flat) - \hat{x}_i(\flat)$, $\tilde{z}_i(\flat) \triangleq z_i(\flat) - \hat{z}_i(\flat)$, the following description is obtained of the estimation error dynamics:

$$\begin{cases} e_i(\flat+1) = (\bar{A}_i(\flat) - S_i(\flat)\bar{C}_i(\flat))e_i(\flat) + \sum_{j=1}^{U} a_{ij}\bar{\Gamma}e_j(\flat) \\ \qquad +\bar{E}_i(\flat)g(\flat, I_A\bar{x}_i(\flat)) + \bar{F}_i(\flat)\bar{w}_i(\flat) \\ \qquad -S_i(\flat)\zeta_i(\flat) - S_i(\flat)h_i(\flat) - S_i(\flat)D_i(\flat)v_i(\flat) \\ \tilde{z}_i(\flat) = \bar{L}_i(\flat)e_i(\flat), \ i = 1, 2, \ldots, U. \end{cases} \tag{11}$$

Define

$$\beth(\flat) \triangleq \left[\beth_1^T(\flat) \ \beth_2^T(\flat) \cdots \beth_U^T(\flat)\right]^T,$$
$$(\beth = \bar{x}, e, \tilde{z}, \zeta, h, v, \bar{w}),$$
$$\bar{g}(\flat, I_B\bar{x}(\flat)) \triangleq \Big[\, g^T(\flat, I_A\bar{x}_1(\flat)) \ g^T(\flat, I_A\bar{x}_2(\flat)) \cdots$$
$$g^T(\flat, I_A\bar{x}_U(\flat))\Big]^T,$$
$$I_B \triangleq I_{(U)} \otimes I_A,$$
$$\daleth(\flat) \triangleq \mathrm{diag}\{\daleth_1(\flat), \daleth_2(\flat), \ldots, \daleth_U(\flat)\},$$
$$(\daleth = \bar{A}, \bar{E}, \bar{F}, D, \bar{C}, S, \bar{L}).$$

We derive the following compact form from (5) and (11):

$$\begin{aligned} \bar{x}(\flat+1) = {} & (\bar{A}(\flat) + \Lambda \otimes \bar{\Gamma})\bar{x}(\flat) + \bar{E}(\flat)\bar{g}(\flat, I_B\bar{x}(\flat)) \\ & + \bar{F}(\flat)\bar{w}(\flat), \end{aligned} \tag{12}$$

and

$$\begin{cases} e(\flat+1) = (\bar{A}(\flat) + \Lambda \otimes \bar{\Gamma} - S(\flat)\bar{C}(\flat))e(\flat) \\ \qquad +\bar{E}(\flat)\bar{g}(\flat, I_B\bar{x}(\flat)) + \bar{F}(\flat)\bar{w}(\flat) \\ \qquad -S(\flat)\zeta(\flat) - S(\flat)h(\flat) - S(\flat)D(\flat)v(\flat), \\ \tilde{z}(\flat) = \bar{L}(\flat)e(\flat). \end{cases} \tag{13}$$

Considering (3), we can yield the statistical characteristics of $\bar{g}(\flat, I_B\bar{x}(\flat))$ as follows:

$$\mathbb{E}\{\bar{g}(\flat, I_B\bar{x}(\flat))|I_B\bar{x}(\flat)\} = 0 \tag{14}$$

$$\mathbb{E}\{\bar{g}(\flat, I_B\bar{x}(\flat))\bar{g}^T(j, I_B\bar{x}(j))|I_B\bar{x}(\flat)\} = 0, \flat \neq j \tag{15}$$

$$\begin{aligned} & \mathbb{E}\{\bar{g}(\flat, I_B\bar{x}(\flat))\bar{g}^T(\flat, I_B\bar{x}(\flat))|I_B\bar{x}(\flat)\} \\ & = \sum_{r=1}^{q}(1_U \otimes \pi_r(\flat))(1_U \otimes \pi_r(\flat))^T\mathbb{E}\{(I_B\bar{x}(\flat))^T \\ & \quad \times (I_{(U)} \otimes \Pi_r(\flat))I_B\bar{x}(\flat)\} \\ & = \sum_{r=1}^{q}(1_U 1_U^T) \otimes \Theta_r(\flat)\mathbb{E}\{(I_B\bar{x}(\flat))^T(I_{(U)} \otimes \Pi_r(\flat))I_B\bar{x}(\flat)\}. \end{aligned} \tag{16}$$

Letting $\eta(\flat) \triangleq \left[\bar{x}^T(\flat) \ e^T(\flat)\right]^T$, the augmented estimation error dynamics is described on the basis of (12)-(13) as follows:

$$\begin{cases} \eta(\flat+1) = \bar{\mathcal{A}}(\flat)\eta(\flat) + \bar{\mathcal{F}}(\flat)\bar{w}(\flat) + \bar{\mathcal{E}}(\flat)\bar{g}(\flat, I_B\bar{x}(\flat)) \\ \qquad -\mathcal{S}(\flat)\zeta(\flat) - \mathcal{S}(\flat)h(\flat) - \mathcal{S}(\flat)D(\flat)v(\flat) \\ \tilde{z}(\flat) = \bar{\mathcal{L}}(\flat)\eta(\flat) \end{cases} \tag{17}$$

where

$$\bar{\mathcal{A}}(\flat) \triangleq \mathrm{diag}\{\bar{A}(\flat) + \Lambda \otimes \bar{\Gamma}, \ \bar{A}(\flat) + \Lambda \otimes \bar{\Gamma} - S(\flat)\bar{C}(\flat)\},$$
$$\mathcal{S}(\flat) \triangleq \begin{bmatrix} 0 \\ S(\flat) \end{bmatrix}, \ \bar{\mathcal{F}}(\flat) \triangleq \begin{bmatrix} \bar{F}(\flat) \\ \bar{F}(\flat) \end{bmatrix}, \ \bar{\mathcal{L}}(\flat) \triangleq \begin{bmatrix} 0 \ \bar{L}(\flat) \end{bmatrix},$$
$$\bar{\mathcal{E}}(\flat) \triangleq \begin{bmatrix} \bar{E}(\flat) \\ \bar{E}(\flat) \end{bmatrix}.$$

The definition of the state covariance matrix for the dynamical system (17) is as follows:

$$\mathbb{L}(\flat) \triangleq \mathbb{E}\{\eta(\flat)\eta^T(\flat)\} = \mathbb{E}\left\{\begin{bmatrix} \bar{x}(\flat) \\ e(\flat) \end{bmatrix}\begin{bmatrix} \bar{x}(\flat) \\ e(\flat) \end{bmatrix}^T\right\}. \tag{18}$$

The objective of this paper is to develop the time-varying state estimator (10) for the CN (1). Specifically, our focus is on determining the gain parameters $S_i(\flat)$ ($i = 1, 2, \ldots, U$, $\flat = 1, 2, \ldots, \mathcal{N} - 1$) that meet both of the following requirements simultaneously:

- $R1$: known the noise rejection level $\gamma > 0$, the matrices $\Omega_w > 0$, $\Omega_\zeta > 0$, $\Omega_h > 0$, $\Omega_v > 0$ and $\Omega_\eta > 0$, and the initial state $\eta(0)$, the estimation error $\tilde{z}(\flat)$ satisfies the performance of H_∞ noise rejection as follow:

$$J_1 \triangleq \mathbb{E}\left\{\sum_{\flat=0}^{\mathcal{N}-1}\left[(\|\tilde{z}(\flat)\|)^2 - \gamma^2(\|\bar{w}(\flat)\|^2_{\Omega_w} + \|\vartheta(\flat)\|^2)\right]\right\} - \gamma^2\mathbb{E}\{\eta^T(0)\Omega_\eta\eta(0)\} < 0 \ \ (\forall \bar{w}(\flat), \vartheta(\flat) \neq 0) \tag{19}$$

  where $\|\bar{w}(\flat)\|^2_{\Omega_w} \triangleq \bar{w}^T(\flat)\Omega_w\bar{w}(\flat)$, $\|\vartheta(\flat)\|^2 \triangleq \zeta^T(\flat)\Omega_\zeta\zeta(\flat) + h^T(\flat)\Omega_h h(\flat) + v^T(\flat)\Omega_v v(\flat)$.
- $R2$: the constraint for the estimation error covariance is specified as follows:

$$J_2 \triangleq \mathbb{E}\left\{e(\flat)e^T(\flat)\right\} \leq \Xi(\flat) \tag{20}$$

  where $\{\Xi(\flat)\}_{1\leq\flat\leq\mathcal{N}+1}$ denotes a sequence of provided matrices that determine the appropriate level of estimation accuracy according to practical needs.

Remark 4: The variance-constrained estimator designed in this paper offers greater flexibility compared to the optimal estimate of the minimum error covariance, which satisfies a predetermined upper bound constraint on the error variance. Moreover, because the variance constraint offers a degree of freedom, other performance requirements can be achieved simultaneously (e.g., robustness [46], [47], the desired H_∞ noise rejection level, passivity constraint, stability, and H_2-performance).

III. MAIN RESULTS

A. ANALYSIS OF H_∞ PERFORMANCE

Lemma 3: For a matrix $\mathcal{P} > 0$, and vectors $\mathscr{M}^T$ and $\mathscr{N}^T$, the inequality:

$$\mathscr{M}^T\mathcal{P}\mathscr{N} + \mathscr{N}^T\mathcal{P}\mathscr{M} \leq \mathscr{M}^T\mathcal{P}\mathscr{M} + \mathscr{N}^T\mathcal{P}\mathscr{N}$$

holds.

Now, we initiate the analysis of the H_∞ performance and establish the sufficient conditions for achieving the performance indices (19) and (20) of the designed estimator (10).

Theorem 1: Let the scalar $\gamma > 0$ and estimator gain $S_i(\flat)$ be known. For the matrices $\Omega_\zeta > 0$, $\Omega_h > 0$, $\Omega_v > 0$, $\Omega_w > 0$ and $\Omega_\eta > 0$, the performance requirement of H_∞ noise rejection denoted in (19) is fulfilled with $\bar{w}(\flat) \neq 0$, if there exist families of matrices $\{P(\flat)\}_{1\leq\flat\leq\mathcal{N}+1} > 0$, such that the following recursive matrix inequality holds:

$$\Phi(\flat) = \text{diag}\{\Phi_1(\flat), \Phi_2(\flat), \Phi_3(\flat), \Phi_4(\flat), \Phi_5(\flat)\} < 0 \tag{21}$$

with the initial condition

$$P(0) \leq \gamma^2\Omega_\eta$$

where

$$\begin{aligned}
\Phi_1(\flat) &\triangleq \bar{\mathcal{A}}^T(\flat)P(\flat+1)\bar{\mathcal{A}}(\flat) - P(\flat) + \bar{\mathcal{L}}^T(\flat)\bar{\mathcal{L}}(\flat) + \sum_{r=1}^{q}\hat{\Pi}_r(\flat) \\
&\quad \times \text{tr}[\bar{\mathcal{E}}^T(\flat)P(\flat+1)\bar{\mathcal{E}}(\flat)(1_U 1_U^T) \otimes \Theta_r(\flat)], \\
\Phi_2(\flat) &\triangleq \bar{\mathcal{F}}^T(\flat)P(\flat+1)\bar{\mathcal{F}}(\flat) - \gamma^2\Omega_w, \\
\Phi_3(\flat) &\triangleq 3\mathcal{S}^T(\flat)P(\flat+1)\mathcal{S}(\flat) - \gamma^2\Omega_\zeta, \\
\Phi_4(\flat) &\triangleq 3\mathcal{S}^T(\flat)P(\flat+1)\mathcal{S}(\flat) - \gamma^2\Omega_h, \\
\Phi_5(\flat) &\triangleq 3D^T(\flat)\mathcal{S}^T(\flat)P(\flat+1)\mathcal{S}(\flat)D(v) - \gamma^2\Omega_v, \\
\hat{\Pi}_r(\flat) &\triangleq \text{diag}\{\tilde{\Pi}_r(\flat), 0\}, \ \tilde{\Pi}_r(\flat) \triangleq I_{(U)} \otimes \text{diag}\{\Pi_r(\flat), 0\}.
\end{aligned}$$

Proof: Denote

$$\mathcal{J}(\flat) \triangleq \eta^T(\flat+1)P(\flat+1)\eta(\flat+1) - \eta^T(\flat)P(\flat)\eta(\flat). \tag{22}$$

Based on (3) and (14), we can acquire that

$$\mathbb{E}\{\bar{g}(\flat, I_B\bar{x}(\flat))|I_B\bar{x}(\flat)\} = 0. \tag{23}$$

By employing Lemma 3, it follows from (17) that:

$$\begin{aligned}
&\mathbb{E}\{\mathcal{J}(\flat)\} \\
&= \mathbb{E}\{\eta^T(\flat)\bar{\mathcal{A}}^T(\flat)P(\flat+1)\bar{\mathcal{A}}(\flat)\eta(\flat) - \eta^T(\flat)P(\flat)\eta(\flat) \\
&\quad + \bar{w}^T(\flat)\bar{\mathcal{F}}^T(\flat)P(\flat+1)\bar{\mathcal{F}}(\flat)\bar{w}(\flat) \\
&\quad + \bar{g}^T(\flat, I_B\bar{x}(\flat))\bar{\mathcal{E}}^T(\flat)P(\flat+1)\bar{\mathcal{E}}(\flat)\bar{g}(\flat, I_B\bar{x}(\flat)) \\
&\quad + \zeta^T(\flat)\mathcal{S}^T(\flat)P(\flat+1)\mathcal{S}(\flat)\zeta(\flat) \\
&\quad + h^T(\flat)\mathcal{S}^T(\flat)P(\flat+1)\mathcal{S}(\flat)h(\flat) \\
&\quad + v^T(\flat)D^T(\flat)\mathcal{S}^T(\flat)P(\flat+1)\mathcal{S}(\flat)D(\flat)v(\flat) \\
&\quad + \zeta^T(\flat)\mathcal{S}^T(\flat)P(\flat+1)\mathcal{S}(\flat)h(\flat) \\
&\quad + \zeta^T(\flat)\mathcal{S}^T(\flat)P(\flat+1)\mathcal{S}(\flat)(\flat)D(\flat)v(\flat) \\
&\quad + h^T(\flat)\mathcal{S}^T(\flat)P(\flat+1)\mathcal{S}(\flat)\zeta(\flat) \\
&\quad + h^T(\flat)\mathcal{S}^T(\flat)P(\flat+1)\mathcal{S}(\flat)D(\flat)v(\flat) \\
&\quad + v^T(\flat)D^T(\flat)\mathcal{S}^T(\flat)P(\flat+1)\mathcal{S}(\flat)\zeta(\flat) \\
&\quad + v^T(\flat)D^T(\flat)\mathcal{S}^T(\flat)P(\flat+1)\mathcal{S}(\flat)h(\flat)\} \\
&\leq \mathbb{E}\{\eta^T(\flat)\bar{\mathcal{A}}^T(\flat)P(\flat+1)\bar{\mathcal{A}}(\flat)\eta(\flat) - \eta^T(\flat)P(\flat)\eta(\flat) \\
&\quad + \bar{w}^T(\flat)\bar{\mathcal{F}}^T(\flat)P(\flat+1)\bar{\mathcal{F}}(\flat)\bar{w}(\flat) \\
&\quad + \bar{g}^T(\flat, I_B\bar{x}(\flat))\bar{\mathcal{E}}^T(\flat)P(\flat+1)\bar{\mathcal{E}}(\flat)\bar{g}(\flat, I_B\bar{x}(\flat)) \\
&\quad + 3\zeta^T(\flat)\mathcal{S}^T(\flat)P(\flat+1)\mathcal{S}(\flat)\zeta(\flat) \\
&\quad + 3h^T(\flat)\mathcal{S}^T(\flat)P(\flat+1)\mathcal{S}(\flat)h(\flat) \\
&\quad + 3v^T(\flat)D^T(\flat)\mathcal{S}^T(\flat)P(\flat+1)\mathcal{S}(\flat)D(\flat)v(\flat)\}.
\end{aligned} \tag{24}$$

Employing the properties of matrix trace and Kronecker product, and considering (16), we have

$$\begin{aligned}
&\mathbb{E}\left\{\bar{g}^T(\flat, I_B\bar{x}(\flat))\bar{\mathcal{E}}^T(\flat)P(\flat+1)\bar{\mathcal{E}}(\flat)\bar{g}(\flat, I_B\bar{x}(\flat))\right\} \\
&= \mathbb{E}\left\{\text{tr}\left[\bar{\mathcal{E}}^T(\flat)P(\flat+1)\bar{\mathcal{E}}(\flat)\bar{g}(\flat, I_B\bar{x}(\flat))\bar{g}^T(\flat, I_B\bar{x}(\flat))\right]\right\} \\
&= \mathbb{E}\left\{\text{tr}\left[\bar{\mathcal{E}}^T(\flat)P(\flat+1)\bar{\mathcal{E}}(\flat)\sum_{r=1}^{q}(1_U \otimes \pi_r(\flat))(1_U \otimes \pi_r(\flat))^T\right.\right.
\end{aligned}$$

$$
\begin{aligned}
&\times (I_B\bar{x}(\flat))^T(I_{(U)}\otimes\Pi_r(\flat))I_B\bar{x}(\flat)\Big]\Big\}\\
&=\mathbb{E}\Big\{\mathrm{tr}\Big[\bar{\mathcal{E}}^T(\flat)P(\flat+1)\bar{\mathcal{E}}(\flat)\sum_{r=1}^{q}(1_U1_U^T)\otimes(\pi_r(\flat)\pi_r^T(\flat))\\
&\times (I_B\bar{x}(\flat))^T(I_{(U)}\otimes\Pi_r(\flat))I_B\bar{x}(\flat)\Big]\Big\}\\
&=\mathbb{E}\Big\{\mathrm{tr}\Big[\bar{\mathcal{E}}^T(\flat)P(\flat+1)\bar{\mathcal{E}}(\flat)\sum_{r=1}^{q}(1_U1_U^T)\otimes\Theta_r(\flat)\\
&\times (I_B\bar{x}(\flat))^T(I_{(U)}\otimes\Pi_r(\flat))I_B\bar{x}(\flat)\Big]\Big\}\\
&=\mathbb{E}\Big\{\mathrm{tr}\Big[\bar{\mathcal{E}}^T(\flat)P(\flat+1)\bar{\mathcal{E}}(\flat)\sum_{r=1}^{q}(1_U1_U^T)\otimes\Theta_r(\flat)\\
&\times \eta^T(\flat)I_C^TI_B^T(I_{(U)}\otimes\Pi_r(\flat))I_BI_C\eta(\flat)\Big]\Big\}\\
&=\mathbb{E}\Big\{\mathrm{tr}\Big[\bar{\mathcal{E}}^T(\flat)P(\flat+1)\bar{\mathcal{E}}(\flat)\sum_{r=1}^{q}(1_U1_U^T)\otimes\Theta_r(\flat)\eta^T(\flat)\\
&\times I_C^T(I_{(U)}\otimes I_A^T)(I_{(U)}\otimes\Pi_r(\flat))(I_{(U)}\otimes I_A)I_C\eta(\flat)\Big]\Big\}\\
&=\mathbb{E}\Big\{\mathrm{tr}\Big[\bar{\mathcal{E}}^T(\flat)P(\flat+1)\bar{\mathcal{E}}(\flat)\sum_{r=1}^{q}(1_U1_U^T)\otimes\Theta_r(\flat)\\
&\times \eta^T(\flat)\hat{\Pi}_r(\flat)\eta(\flat)\Big]\Big\}\\
&=\mathbb{E}\Big\{\sum_{r=1}^{q}\mathrm{tr}\Big[\bar{\mathcal{E}}^T(\flat)P(\flat+1)\bar{\mathcal{E}}(\flat)(1_U1_U^T)\otimes\Theta_r(\flat)\Big]\\
&\times \eta^T(\flat)\hat{\Pi}_r(\flat)\eta(\flat)\Big\}\\
&=\mathbb{E}\Big\{\eta^T(\flat)\sum_{r=1}^{q}\hat{\Pi}_r(\flat)\\
&\times \mathrm{tr}\Big[\bar{\mathcal{E}}^T(\flat)P(\flat+1)\bar{\mathcal{E}}(\flat)(1_U1_U^T)\otimes\Theta_r(\flat)\Big]\eta(\flat)\Big\} \qquad (25)
\end{aligned}
$$

where $I_C \triangleq \big[I_{(U(l_x+l_b))}\ 0\big]$.

Adding the zero term $\tilde{z}^T(\flat)\tilde{z}(\flat) - \gamma^2\|\vartheta(\flat)\|^2 - \gamma^2\bar{w}^T(\flat)\Omega_w\bar{w}(\flat) - \tilde{z}^T(\flat)\tilde{z}(\flat) + \gamma^2\|\vartheta(\flat)\|^2 + \gamma^2\bar{w}^T(\flat)\Omega_w\bar{w}(\flat)$ to $\mathbb{E}\{\mathcal{J}(\flat)\}$, the following inequality is obtained:

$$
\begin{aligned}
\mathbb{E}\{\mathcal{J}(\flat)\} \le \mathbb{E}\Big\{&\aleph^T(\flat)\Phi(\flat)\aleph(\flat) - \tilde{z}^T(\flat)\tilde{z}(\flat)\\
&+\gamma^2\|\vartheta(\flat)\|^2 + \gamma^2\bar{w}^T(\flat)\Omega_w\bar{w}(\flat)\Big\} \qquad (26)
\end{aligned}
$$

where $\aleph(\flat) \triangleq \big[\eta^T(\flat)\ \bar{w}^T(\flat)\ \zeta^T(\flat)\ h^T(\flat)\ v^T(\flat)\big]^T$. Noticing (26), it is deduced that

$$
\begin{aligned}
&\sum_{\flat=0}^{\mathcal{N}-1}\mathbb{E}\{\mathcal{J}(\flat)\}\\
&\quad=\mathbb{E}\{\eta^T(\mathcal{N})P(\mathcal{N})\eta(\mathcal{N}) - \eta^T(0)P(0)\eta(0)\}\\
&\quad\le \sum_{\flat=0}^{\mathcal{N}-1}\mathbb{E}\Big\{\aleph^T(\flat)\Phi(\flat)\aleph(\flat) - (\tilde{z}^T(\flat)\tilde{z}(\flat)\\
&\qquad -\gamma^2\|\vartheta(\flat)\|^2 - \gamma^2\bar{w}^T(\flat)\Omega_w\bar{w}(\flat))\Big\}. \qquad (27)
\end{aligned}
$$

Consequently, the performance index in (19) can be rephrased in the following form:

$$
\begin{aligned}
J_1 \le \mathbb{E}\left\{\sum_{\flat=0}^{\mathcal{N}-1}\aleph^T(\flat)\Phi(\flat)\aleph(\flat)\right\} &+ \eta^T(0)\left(P(0)-\gamma^2\Omega_\eta\right)\eta(0)\\
&-\mathbb{E}\{\eta^T(\mathcal{N})P(\mathcal{N})\eta(\mathcal{N})\}. \qquad (28)
\end{aligned}
$$

According to the initial condition $P(0) \le \gamma^2\Omega_\eta$ and the condition $\Phi(\flat) < 0$ and $P(\mathcal{N}) > 0$, it follows from (28) that $J_1 < 0$, and the proof of this theorem is complete. ■

B. ANALYSIS OF VARIANCE-CONSTRAINED PERFORMANCE

In this subsection, our purpose is to investigate the variance-constrained performance of estimator (10) for CN (1).

Theorem 2: Consider the CN (1), and let the gain $S_i(\flat)$ be known. We can acquire $\mathbb{L}(\flat) \le \mathcal{R}(\flat)$ ($\forall\flat \in 1, 2, \cdots, \mathcal{N}+1$), if there exist families of matrices $\{\mathcal{R}(\flat)\}_{1\le\flat\le\mathcal{N}+1} > 0$ meeting the following RMI:

$$
\mathcal{R}(\flat+1) \ge \Psi(\mathcal{R}(\flat)) \qquad (29)
$$

with the initial condition

$$
\mathcal{R}(0) = \mathbb{L}(0)
$$

where

$$
\begin{aligned}
\Psi(\mathcal{R}(\flat)) \triangleq\ &\bar{\mathcal{A}}(\flat)\mathcal{R}(\flat)\bar{\mathcal{A}}^T(\flat) + \bar{\mathcal{F}}(\flat)W\bar{\mathcal{F}}^T(\flat)\\
&+3\mathcal{S}(\flat)D(\flat)V_0D^T(\flat)\mathcal{S}^T(\flat) + 3\mathcal{S}(\flat)H_0\mathcal{S}^T(\flat)\\
&+3\mathcal{S}(\flat)\mathscr{Z}_0\mathcal{S}^T(\flat) + \sum_{r=1}^{q}\bar{\mathcal{E}}(\flat)(1_U1_U^T)\otimes\Theta_r(\flat)\\
&\times\bar{\mathcal{E}}^T(\flat)\mathrm{tr}[\hat{\Pi}_r(\flat)\mathcal{R}(\flat)],\\
W \triangleq I_{(U)}\otimes &\mathrm{diag}\{w_0^2, \beta_0^2\},\ \ V_0 \triangleq I_{(U)}\otimes v_0^2,\\
H_0 \triangleq I_{(U)}\otimes &h_0^2,\ \ \mathscr{Z}_0 \triangleq I_{(U)}\otimes\frac{\varrho^2}{4}.
\end{aligned}
$$

Proof: According to (17), the Lyapunov-type equation that governs the evolution of covariance $\mathbb{L}(\flat)$ can be expressed in the following form:

$$
\begin{aligned}
\mathbb{L}(\flat+1) = \mathbb{E}&\left\{\eta(\flat+1)\eta^T(\flat+1)\right\}\\
\le \mathbb{E}\{&\bar{\mathcal{A}}(\flat)\eta(\flat)\eta^T(\flat)\bar{\mathcal{A}}^T(\flat) + \bar{\mathcal{F}}(\flat)\bar{w}(\flat)\bar{w}^T(\flat)\bar{\mathcal{F}}^T(\flat)\\
&+\bar{\mathcal{E}}(\flat)\bar{g}(\flat, I_B\bar{x}(\flat))\bar{g}^T(\flat, I_B\bar{x}(\flat))\bar{\mathcal{E}}^T(\flat)\\
&+3\mathcal{S}(\flat)\zeta(\flat)\zeta^T(\flat)\mathcal{S}^T(\flat)\\
&+3\mathcal{S}(\flat)h(\flat)h^T(\flat)\mathcal{S}^T(\flat)\\
&+3\mathcal{S}(\flat)D(\flat)v(\flat)v^T(\flat)D^T(\flat)\mathcal{S}^T(\flat)\}. \qquad (30)
\end{aligned}
$$

In terms of (16), one has

$$\begin{aligned}
&\mathbb{E}\left\{\bar{\mathcal{E}}(\flat)\bar{g}(\flat, I_B\bar{x}(\flat))\bar{g}^T(\flat, I_B\bar{x}(\flat))\bar{\mathcal{E}}^T(\flat)\right\} \\
&= \bar{\mathcal{E}}(\flat)\sum_{r=1}^{q}(1_U 1_U^T)\otimes\Theta_r(\flat)\mathbb{E}\big\{(I_B\bar{x}(\flat))^T(I_{(U)}\otimes\Pi_r(\flat)) \\
&\quad\times I_B\bar{x}(\flat)\big\}\bar{\mathcal{E}}^T(\flat) \\
&= \sum_{r=1}^{q}\bar{\mathcal{E}}(\flat)(1_U 1_U^T)\otimes\Theta_r(\flat)\bar{\mathcal{E}}^T(\flat)\cdot\mathrm{tr}[\hat{\Pi}_r(\flat)\mathbb{L}(\flat)]. \qquad (31)
\end{aligned}$$

We can obtain

$$\begin{aligned}
\mathbb{L}(\flat+1) \leq\ & \bar{\mathcal{A}}(\flat)\mathbb{L}(\flat)\bar{\mathcal{A}}^T(\flat) + \bar{\mathcal{F}}(\flat)W\bar{\mathcal{F}}^T(\flat) \\
& + 3\mathcal{S}(\flat)D(\flat)V_0D^T(\flat)\mathcal{S}^T(\flat) + 3\mathcal{S}(\flat)H_0\mathcal{S}^T(\flat) \\
& + 3\mathcal{S}(\flat)\mathscr{Z}_0\mathcal{S}^T(\flat) + \sum_{r=1}^{q}\bar{\mathcal{E}}(\flat)(1_U 1_U^T)\otimes\Theta_r(\flat) \\
& \times\bar{\mathcal{E}}^T(\flat)\mathrm{tr}[\hat{\Pi}_r(\flat)\mathbb{L}(\flat)] \\
=\ & \Psi(\mathbb{L}(\flat)). \qquad (32)
\end{aligned}$$

Now we begin to conduct the proof using the mathematical induction method. Clearly, we yield $\mathcal{R}(0) \geq \mathbb{L}(0)$ according to the initial condition easily. Setting $\mathcal{R}(\flat) \geq \mathbb{L}(\flat)$, we can obtain the inequalities as indicated below:

$$\mathcal{R}(\flat+1) \geq \Psi(\mathcal{R}(\flat)) \geq \Psi(\mathbb{L}(\flat)) \geq \mathbb{L}(\flat+1), \qquad (33)$$

the proof is now complete. ■

We can get Corollary 1 easily from Theorem 2.

Corollary 1: The following inequality holds:

$$\begin{aligned}
\mathbb{E}\left\{e(\flat)e^T(\flat)\right\} &= \left[0\ I_{(U(l_x+l_b))}\right]\mathbb{L}(\flat)\left[0\ I_{(U(l_x+l_b))}\right]^T \\
&\leq \left[0\ I_{(U(l_x+l_b))}\right]\mathcal{R}(\flat)\left[0\ I_{(U(l_x+l_b))}\right]^T, \ \forall\flat.
\end{aligned}$$

To sum up the previous analysis, we present Theorem 3, which takes both performance requirements (H_∞ noise rejection (19) and the prescribed upper bound on the SE error variance (20)) into account under a unified framework by utilizing the linear matrix inequality (LMI) approach.

Theorem 3: Considering the CN (1), for a constant $\gamma > 0$, matrices $\Omega_w > 0$, $\Omega_\zeta > 0$, $\Omega_h > 0$, $\Omega_v > 0$, $\Omega_\eta > 0$, and error variance upper bounds $\{\Xi(\flat) > 0\}_{1\leq\flat\leq\mathcal{N}+1}$, the variance-constrained H_∞ state estimator (10) exists if families of matrices $\{P(\flat)\}_{1\leq\flat\leq\mathcal{N}+1} > 0$, and $\{\mathcal{R}(\flat)\}_{1\leq\flat\leq\mathcal{N}+1} > 0$, and scalars $\{\wp_r(\flat)\}_{0\leq\flat\leq\mathcal{N}} > 0$ $(r = 1, 2, \ldots q)$ exist fulfilling the following RMIs:

$$\begin{bmatrix} -\wp_r(\flat) & * \\ \bar{\mathcal{E}}(\flat)(1_U\otimes\pi_r(\flat)) & -\bar{P}(\flat+1)\end{bmatrix} < 0, \qquad (34)$$

$$\begin{bmatrix} \Upsilon_1(\flat) & * \\ \Upsilon_2(\flat) & \Upsilon_3(\flat+1)\end{bmatrix} < 0, \qquad (35)$$

$$\begin{bmatrix} -\mathcal{R}(\flat+1) & * \\ \Upsilon_5(\flat) & \Upsilon_6(\flat)\end{bmatrix} < 0, \qquad (36)$$

$$\mathcal{R}_2(\flat+1) - \Xi(\flat+1) < 0, \qquad (37)$$

with the initial conditions

$$\begin{cases} P(0) \leq \gamma^2\Omega_\eta \\ \mathcal{R}(0) = \mathbb{L}(0) \\ \mathbb{E}\left\{e(0)e^T(0)\right\} = \mathcal{R}_2(0) \leq \Xi(0) \end{cases} \qquad (38)$$

and parameter update

$$P(\flat+1) \triangleq \bar{P}^{-1}(\flat+1) \qquad (39)$$

where

$$\begin{aligned}
\Upsilon_1(\flat) &\triangleq \mathrm{diag}\big\{\Upsilon_{11}(\flat), -\gamma^2\Omega_w, -\gamma^2\Omega_\zeta, -\gamma^2\Omega_h, -\gamma^2\Omega_v\big\}, \\
\Upsilon_{11}(\flat) &\triangleq \sum_{r=1}^{q}\hat{\Pi}_r(\flat)\wp_r(\flat) - P(\flat), \\
\Upsilon_2(\flat) &\triangleq \begin{bmatrix} \bar{\mathcal{A}}(\flat) & 0 & 0 & 0 & 0 \\ \bar{\mathcal{L}}(\flat) & 0 & 0 & 0 & 0 \\ 0 & \bar{\mathcal{F}}(\flat) & 0 & 0 & 0 \\ 0 & 0 & \sqrt{3}\mathcal{S}(\flat) & 0 & 0 \\ 0 & 0 & 0 & \sqrt{3}\mathcal{S}(\flat) & 0 \\ 0 & 0 & 0 & 0 & \Upsilon_{265}(\flat)\end{bmatrix}, \\
\bar{\mathcal{A}}(\flat) &\triangleq \check{\mathcal{A}}_1(\flat) + \check{\mathcal{A}}_2(\flat), \ \Upsilon_{265}(\flat) \triangleq \sqrt{3}\mathcal{S}(\flat)D(\flat), \\
\check{\mathcal{A}}_1(\flat) &\triangleq \mathrm{diag}\{\bar{A}(\flat) + \Lambda\otimes\bar{\Gamma}, \bar{A}(\flat) + \Lambda\otimes\bar{\Gamma}\}, \\
\check{\mathcal{A}}_2(\flat) &\triangleq \mathrm{diag}\{0, -S(\flat)\bar{C}(\flat)\}, \\
\Upsilon_3(\flat+1) &\triangleq \mathrm{diag}\big\{-\bar{P}(\flat+1), -I_{(l_zU)}, -\bar{P}(\flat+1), \\
&\qquad -\bar{P}(\flat+1), -\bar{P}(\flat+1), -\bar{P}(\flat+1)\big\}, \\
\Upsilon_5(\flat) &\triangleq \begin{bmatrix} \mathcal{R}(\flat)\bar{\mathcal{A}}^T(\flat) \\ \bar{\mathcal{F}}^T(\flat) \\ \sqrt{3}D^T(\flat)\mathcal{S}^T(\flat) \\ \sqrt{3}\mathcal{S}^T(\flat) \\ \sqrt{3}\mathcal{S}^T(\flat) \\ \Upsilon_{56}(\flat)\end{bmatrix}, \\
\Upsilon_6(\flat) &\triangleq \mathrm{diag}\big\{-\mathcal{R}(\flat), -W^{-1}, -V_0^{-1}, -H_0^{-1}, \\
&\qquad -\mathscr{Z}_0^{-1}, -\Upsilon_{66}(\flat)\big\}, \\
V_0 &\triangleq v_0^2, \ H_0 \triangleq h_0^2, \ \mathscr{Z}_0 \triangleq \frac{\varrho^2}{4}, \\
\Upsilon_{56}(\flat) &\triangleq [\bar{\mathcal{E}}(\flat)(1_U\otimes\pi_1(\flat)), \ldots, \bar{\mathcal{E}}(\flat)(1_U\otimes\pi_q(\flat))]^T, \\
\Upsilon_{66}(\flat) &\triangleq \mathrm{diag}\big\{\varphi_1(\flat), \varphi_2(\flat), \ldots, \varphi_q(\flat)\big\}, \\
\varphi_r(\flat) &\triangleq \mathrm{tr}[\hat{\Pi}_r(\flat)\mathcal{R}(\flat)]^{-1}, \ (r = 1, 2, \ldots, q)
\end{aligned}$$

Proof: Through utilizing the Schur Complement Lemma, (34) holds if and only if the following inequality holds:

$$\begin{aligned}
&(1_U\otimes\pi_r(\flat))^T\bar{\mathcal{E}}^T(\flat)P(\flat+1)\bar{\mathcal{E}}(\flat)(1_U\otimes\pi_r(\flat)) \\
&\quad < \wp_r(\flat), \ (r = 1, 2, \ldots, q). \qquad (40)
\end{aligned}$$

In addition, with the property of matrix trace, we can rephrase (40) as

$$\begin{aligned}
&\mathrm{tr}[(1_U\otimes\pi_r(\flat))^T\bar{\mathcal{E}}^T(\flat)P(\flat+1)\bar{\mathcal{E}}(\flat)(1_U\otimes\pi_r(\flat))] \\
&= \mathrm{tr}[\bar{\mathcal{E}}^T(\flat)P(\flat+1)\bar{\mathcal{E}}(\flat)(1_U\otimes\pi_r(\flat))(1_U\otimes\pi_r(\flat))^T] \\
&= \mathrm{tr}[\bar{\mathcal{E}}^T(\flat)P(\flat+1)\bar{\mathcal{E}}(\flat)(1_U 1_U^T)\otimes(\pi_r(\flat)\pi_r^T(\flat))]
\end{aligned}$$

$$
\begin{aligned}
&= \mathrm{tr}[\bar{\mathcal{E}}^T(\flat)P(\flat+1)\bar{\mathcal{E}}(\flat)(1_U 1_U^T)\otimes\Theta_r(\flat)] \\
&< \mathrm{tr}[\wp_r(\flat)] \\
&= \wp_r(\flat),\ \ (r=1,2,\ldots,q). \qquad (41)
\end{aligned}
$$

By virtue of Schur Complement Lemma, we yield that (35) holds as long as the following inequality holds:

$$\Phi(\flat) = \mathrm{diag}\{\bar{\Phi}_1(\flat), \Phi_2(\flat), \Phi_3(\flat), \Phi_4(\flat), \Phi_5(\flat)\} < 0 \quad (42)$$

where

$$
\begin{aligned}
\bar{\Phi}_1(\flat) \triangleq\ & \bar{\mathcal{A}}^T(\flat)P(\flat+1)\bar{\mathcal{A}}(\flat)+\bar{\mathcal{L}}^T(\flat)\bar{\mathcal{L}}(\flat)-P(\flat) \\
&+\sum_{r=1}^{q}\hat{\Pi}_r(\flat)\wp_r(\flat).
\end{aligned}
$$

On the basis of (41) and (42), (21) can be derived easily. Hence, if (34) and (35) hold, then (21) holds.

By the same method, we can easily acquire that (29) holds if and only if (36) holds. Thus, on the basis of Theorems 1-2 and Corollary 1, it can be concluded that the H_∞ performance constraint defined in (19) is satisfied, in the meantime, the estimation error of CN (1) achieves $\mathbb{E}\{e(\flat)e^T(\flat)\} \le [0\ I_{(U(l_x+l_b))}]\,\mathcal{R}(\flat)\,[0\ I_{(U(l_x+l_b))}]^T$.

Let the variable $\mathcal{R}(\flat)$ be decomposed in the following form:

$$\mathcal{R}(\flat) = \begin{bmatrix}\mathcal{R}_1(\flat) & * \\ \mathcal{R}_3(\flat) & \mathcal{R}_2(\flat)\end{bmatrix}. \quad (43)$$

From (37) and (43), it is evident that

$$
\begin{aligned}
\mathbb{E}\{e(\flat)e^T(\flat)\} &\le [0\ I_{(U(l_x+l_b))}]\,\mathcal{R}(\flat)\,[0\ I_{(U(l_x+l_b))}]^T \\
&= \mathcal{R}_2(\flat) \\
&< \Xi(\flat),\ \ (\forall\flat\in\{0,1,\ldots,\mathcal{N}+1\}), \qquad (44)
\end{aligned}
$$

which completes this proof. ■

In accordance with Theorem 3, we can sum up the H_∞ variance-constrained estimator design (*HVED*) algorithm as follows.

Remark 5: Until now, the major work of this paper is accomplished and, comparing to existing literature, the distinctive merits of the main results in this paper are highlighted as follows: 1) both the system state and the dynamical bias are simultaneously estimated for a class of nonlinear time-varying complex networks under BESs; 2) performance analysis is achieved of both the H_∞ noise rejection and the prescribed upper bound constraint on the SE error variance by resorting to stochastic analysis and matrix inequalities technique; and 3) sufficient conditions are brought forward for the existence of the variance-constrained H_∞ state estimator, based on which the estimator gains are readily computed.

IV. ILLUSTRATIVE EXAMPLE

In this section, the correctness of the developed estimation algorithm is testified via a numerical simulation example.

Consider the time-varying CN (1) ($U = 3$), whose parameters are given as follows [16]:

$$\alpha_1=\alpha_2=0.5,\ w_0^2=v_0^2=\beta_0^2=0.04,\ M=6,$$

Algorithm 1 *HVED*

Step 1. Given the H_∞ performance index γ, the matrices $\Omega_w > 0$, $\Omega_v > 0$, $\Omega_\zeta > 0$ and $\Omega_h > 0$, and the initial conditions $\bar{x}_i(0)$ and $\hat{x}_i(0)$, and select the matrices $\{P(0), \mathcal{R}_2(0)\}$ which satisfy the initial condition (38).

Step 2. Acquire the values of matrices $\{P(\flat+1), \mathcal{R}_2(\flat+1)\}$ and estimator gains $\mathcal{S}(\flat)$ at the sampling instant $\flat$ by solving the LMIs (34)-(37).

Step 3. Set $\flat=\flat+1$ and update parameters $P(\flat)$ and $\mathcal{R}_2(\flat)$.

Step 4. If $\flat<\mathcal{N}$, then go to Step 2, else go to Step 5.

Step 5. Stop.

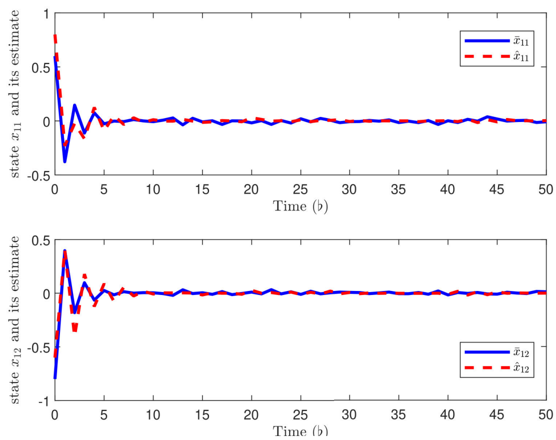

FIGURE 1. $x_1(\flat)$ and its estimate.

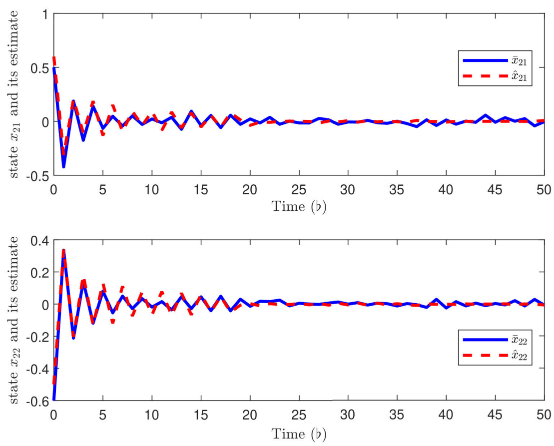

FIGURE 2. $x_2(\flat)$ and its estimate.

$$
\begin{aligned}
&\gamma=0.9,\ p=0.01,\ \varrho=0.03,\ \Omega_w=\mathrm{diag}\{1,1\}, \\
&\Omega_h=\Omega_v=\Omega_\zeta=I,\ \Xi(\flat)=I_{(3)}\otimes\mathrm{diag}\{0.8,0.8\}, \\
&a_{ii}=-0.2,\ a_{ij}=0.1\ (i,j=1,2,3),\ \xi_0^2=1, \\
&A_1(\flat)=\begin{bmatrix}0.4+0.1\sin(\flat) & 0.6 \\ 0.3 & -0.2\end{bmatrix},
\end{aligned}
$$

TABLE 1. Variance-constrained state estimator gain parameters.

$\flat$	0	1	2	3	4	5	6	7	…
$S_1(\flat)$	$\begin{bmatrix}-0.0027\\-0.0027\\-0.0246\\0.2954\end{bmatrix}$	$\begin{bmatrix}-0.8531\\-0.6090\\0.2388\\0.6575\end{bmatrix}$	$\begin{bmatrix}-0.7657\\-0.7042\\0.0170\\0.6233\end{bmatrix}$	$\begin{bmatrix}0.0085\\-0.0530\\-0.0411\\0.3506\end{bmatrix}$	$\begin{bmatrix}-0.0053\\-0.0085\\0.0116\\0.3609\end{bmatrix}$	$\begin{bmatrix}-0.1238\\-0.1251\\-0.1159\\0.4492\end{bmatrix}$	$\begin{bmatrix}-0.2599\\-0.3531\\0.0418\\0.3735\end{bmatrix}$	$\begin{bmatrix}0.0046\\-0.0403\\0.1306\\0.3532\end{bmatrix}$	…
$S_2(\flat)$	$\begin{bmatrix}0.0014\\0.0003\\0.1148\\0.1959\end{bmatrix}$	$\begin{bmatrix}-0.0024\\-0.0028\\0.0976\\0.2433\end{bmatrix}$	$\begin{bmatrix}-0.1191\\-0.1087\\-0.0024\\0.3361\end{bmatrix}$	$\begin{bmatrix}0.0540\\-0.0781\\-0.1426\\0.2589\end{bmatrix}$	$\begin{bmatrix}0.0024\\0.0059\\-0.2249\\0.2831\end{bmatrix}$	$\begin{bmatrix}-0.0125\\-0.0007\\-0.1187\\0.3273\end{bmatrix}$	$\begin{bmatrix}-0.0042\\-0.0058\\0.1429\\0.2318\end{bmatrix}$	$\begin{bmatrix}0.0030\\-0.0052\\0.1309\\0.3379\end{bmatrix}$	…
$S_3(\flat)$	$\begin{bmatrix}-0.0778\\0.2858\\-0.0455\\-0.0017\end{bmatrix}$	$\begin{bmatrix}-0.0147\\-0.0557\\-0.0002\\0.0003\end{bmatrix}$	$\begin{bmatrix}0.0297\\-0.0719\\0.0323\\0.0005\end{bmatrix}$	$\begin{bmatrix}0.0152\\0.0500\\0.0008\\0.0233\end{bmatrix}$	$\begin{bmatrix}0.0041\\-0.0363\\-0.0007\\0.0009\end{bmatrix}$	$\begin{bmatrix}-0.0193\\-0.0335\\0.0012\\0.3609\end{bmatrix}$	$\begin{bmatrix}0.0326\\0.0654\\-0.0002\\-0.0002\end{bmatrix}$	$\begin{bmatrix}0.0032\\-0.0202\\-0.0004\\0.0035\end{bmatrix}$	…

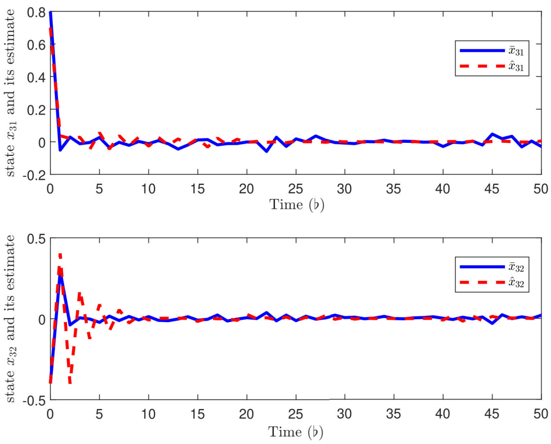

FIGURE 3. $x_3(\flat)$ and its estimate.

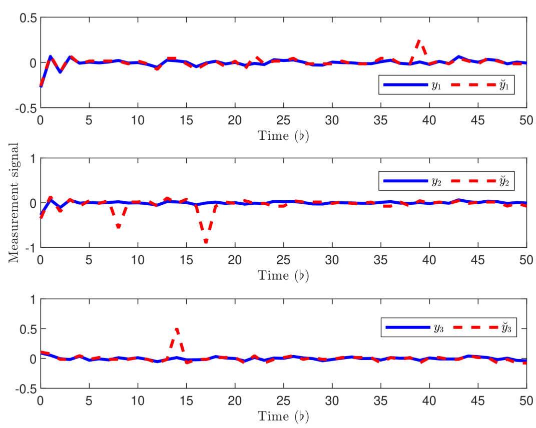

FIGURE 4. The measurement output and the estimator input.

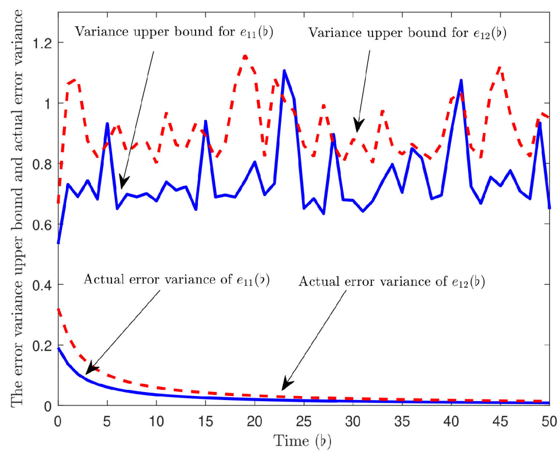

FIGURE 5. Actual error variance of $e_1(\flat)$ and its upper bound.

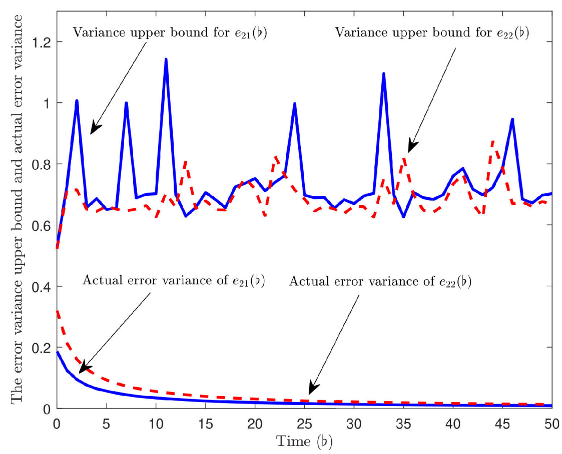

FIGURE 6. Actual error variance of $e_2(\flat)$ and its upper bound.

$$A_2(\flat) = \begin{bmatrix} 0.5 + 0.1\sin(3\flat) & 0.8 \\ 0.4 & -0.2 \end{bmatrix},$$

$$A_3(\flat) = \begin{bmatrix} 0.4 + 0.2\sin(\flat) & 0.5 \\ 0.3 & -0.2 \end{bmatrix},$$

$$B_1(\flat) = \begin{bmatrix} 0.3 & 0.24\sin(\flat) \\ -0.2 & 0.1 \end{bmatrix},$$

$$B_2(\flat) = B_3(\flat) = \begin{bmatrix} 0.4 & 0.1\sin(2\flat) \\ -0.2 & 0.1 \end{bmatrix},$$

$$C_1(\flat) = \begin{bmatrix} 0.99 & 0.15\sin(\flat) \end{bmatrix},$$

$$C_2(\flat) = C_3(\flat) = \begin{bmatrix} 0.95 & 0.25\sin(2\flat) \end{bmatrix},$$

$$D_1(\flat) = D_2(\flat) = D_3(\flat) = \begin{bmatrix} \sin(0.9\flat) \end{bmatrix},$$

$$E_1(\flat) = E_2(\flat) = E_3(\flat) = \begin{bmatrix} 1 + \sin(\flat) & 0 \\ 0 & 1 \end{bmatrix},$$

$$F_1(\flat) = \begin{bmatrix} \sin(0.7\flat) \\ -0.2 \end{bmatrix}, \; F_2(\flat) = \begin{bmatrix} \sin(0.8\flat) \\ -0.2 \end{bmatrix},$$

$$F_3(\flat) = \begin{bmatrix} \sin(0.9\flat) \\ -0.2 \end{bmatrix}, \; G_1(\flat) = \begin{bmatrix} 0.71 & 0.72 \\ -0.7 & 0.6\sin(\flat) \end{bmatrix},$$

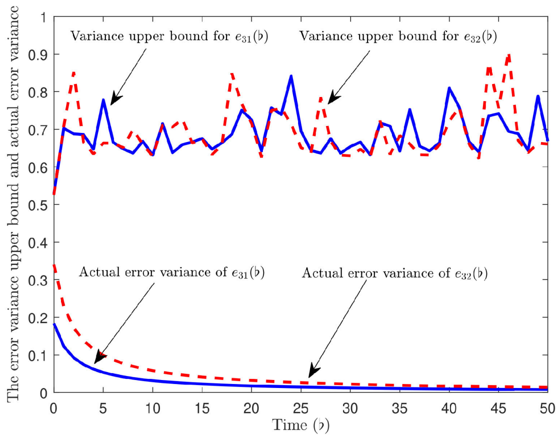

FIGURE 7. Actual error variance of $e_3(\flat)$ and its upper bound.

$$G_2(\flat) = G_3(\flat) = \begin{bmatrix} 0.75 & 0.78 \\ -0.8 & 0.5\sin(\flat) \end{bmatrix},$$
$$H_1(\flat) = H_2(\flat) = \begin{bmatrix} 1 \\ \sin(\flat) \end{bmatrix},\ H_3(\flat) = \begin{bmatrix} 1 \\ \cos(\flat) \end{bmatrix},$$
$$L_1(\flat) = \begin{bmatrix} 0.3 & -0.5\sin(2\flat) \end{bmatrix},$$
$$L_2(\flat) = \begin{bmatrix} 0.5 & -0.4\sin(2\flat) \end{bmatrix},$$
$$L_3(\flat) = \begin{bmatrix} 0.4 & -0.5\sin(2\flat) \end{bmatrix}.$$

Let the stochastic nonlinear function $g(\flat, x_i(\flat))$ be given as follows:

$$g(\flat, x_i(\flat)) = \begin{bmatrix} 0.01 & 0.03 \end{bmatrix}^T \times (0.2x_{i1}(\flat)\xi_1(\flat) + 0.3x_{i2}(\flat)\xi_2(\flat))$$

where $x_{in}(\flat)(n = 1, 2)$ represents the nth element of $x_i(\flat)$, and $\xi_n(\flat)(n = 1, 2)$ are independent bounded stochastic noise sequences with $\mathbb{E}\{\xi_n(\flat)\} = 0$ and variance $\mathbb{V}\{\xi_n(\flat)\} = \xi_0^2$. We can see $g(\flat, x_i(\flat))$ satisfies

$$\mathbb{E}\{g(\flat, x_i(\flat))|x_i(\flat)\} = 0$$
$$\mathbb{E}\{g(\flat, x_i(\flat))g^T(\flat, x_i(\flat))|x_i(\flat)\} = \begin{bmatrix} 0.01 \\ 0.03 \end{bmatrix} \begin{bmatrix} 0.01 \\ 0.03 \end{bmatrix}^T \mathbb{E}\left\{ x_i^T(\flat) \begin{bmatrix} 0.04 & 0 \\ 0 & 0.09 \end{bmatrix} x_i(\flat) \right\}.$$

By solving RMIs (34)-(37), gain parameters of estimator (10) can be acquired which are shown in Table 1:

Let the initial states be selected as follows:

$$\bar{x}_1(0) = \begin{bmatrix} 0.6 \\ -0.8 \\ 0 \\ 0 \end{bmatrix},\ \bar{x}_2(0) = \begin{bmatrix} 0.5 \\ -0.6 \\ 0 \\ 0 \end{bmatrix},\ \bar{x}_3(0) = \begin{bmatrix} 0.8 \\ -0.4 \\ 0 \\ 0 \end{bmatrix},$$
$$\hat{x}_1(0) = \begin{bmatrix} 0.4 \\ -0.3 \\ 0 \\ 0 \end{bmatrix},\ \hat{x}_2(0) = \begin{bmatrix} 0.3 \\ -0.25 \\ 0 \\ 0 \end{bmatrix},\ \hat{x}_3(0) = \begin{bmatrix} 0.35 \\ -0.2 \\ 0 \\ 0 \end{bmatrix}.$$

The results of numerical simulation are depicted in Figs. 1-7. Figs. 1-3 plot the system state $x_i(\flat)$ $(i = 1, 2, 3)$ and their corresponding estimates, respectively. It is seen from Figs. 1-3 that the estimation error is small, and the state estimate is accurate with the noise influence being restrained. That is, the H_∞ noise rejection constraint (19) is achieved. Fig. 4 draws the ideal measurement output and the real measurement signal received by the estimator. In Fig. 4, the obvious deviations between $y_i(\flat)$ and $\check{y}_i(\flat)$ indicate the occurrence of random bit errors during the transmission process. That is, $\check{y}_1(39)$, $\check{y}_2(8)$, $\check{y}_2(17)$ and $\check{y}_3(14)$ are affected by random bit errors, and deviate largely from the ideal measurement signal. Figs. 5-7 illustrate the upper bound on the variance of $e_1(\flat)$, $e_2(\flat)$ and $e_3(\flat)$, as well as the corresponding actual error variance. In Figs. 5-7, the actual error variance is always smaller than the corresponding variance upper bound, which indicates that the upper bound constraint (20) is fulfilled on the SE error variance. Based on the above-mentioned results, it is shown that the proposed HVED algorithm is valid.

V. CONCLUSION

In this article, the finite-horizon H_∞ SE issue has been investigated for a type of time-varying CNs affected by dynamical bias under BESs. The influence of dynamical bias has been involved, which is modeled by a dynamic equation. The BESs have been employed in the transmission process of measurement signals to the estimator, and the occurrence of bit errors, represented by Bernoulli random variables, has been considered. Sufficient conditions have been established to ensure that the estimation error dynamics satisfies the variance constraints and H_∞ noise rejection performance. The designed estimator gain parameter matrices have been obtained by calculating the proposed RMIs. Finally, the correctness and the feasibility of the constructed estimator have been testified by a numerical example. Furthermore, future research aims to extend the findings of this paper to address other issues that involve using BESs such as recursive filtering [48], [49], [50], security-guaranteed analysis [51], [52], fault-tolerant control [53], [54], set-membership filtering [55], [56] or distributed fusion filtering [57], [58].

REFERENCES

[1] E. R. Pinto, E. G. Nepomuceno, and A. S. L. O. Campanharo, "Individual-based modelling of animal brucellosis spread with the use of complex networks," *Int. J. Netw. Dynam. Int.*, vol. 1, no. 1, pp. 120–129, 2022.
[2] J. Suo and N. Li, "Observer-based synchronisation control for discrete-time delayed switched complex networks with coding–decoding approach," *Int. J. Syst. Sci.*, vol. 53, no. 13, pp. 2711–2728, Oct. 2022.
[3] A. Hongsri, T. Botmart, and W. Weera, "Improved on extended dissipative analysis for sampled-data synchronization of complex dynamical networks with coupling delays," *IEEE Access*, vol. 10, pp. 108625–108640, 2022.
[4] R. Sakthivel, N. B. Devi, Y.-K. Ma, and S. Harshavarthini, "State estimation-based hybrid-triggered controller design for synchronization of repeated scalar nonlinear complex dynamical networks," *IEEE Access*, vol. 11, pp. 42069–42081, 2023.
[5] L. Zou, Z. Wang, J. Hu, and H. Dong, "Partial-node-based state estimation for delayed complex networks under intermittent measurement outliers: A multiple-order-holder approach," *IEEE Trans. Neural Netw. Learn. Syst.*, vol. 34, no. 10, pp. 7181–7195, Oct. 2023.
[6] S. Jeong and J. Ban, "Robust dynamic output feedback event-triggering synchronization for complex dynamical networks," *IEEE Access*, vol. 10, pp. 51261–51271, 2022.

[7] D. Liu, Z. Wang, Y. Liu, F. E. Alsaadi, and F. E. Alsaadi, "Recursive state estimation for stochastic complex networks under round-robin communication protocol: Handling packet disorders," *IEEE Trans. Netw. Sci. Eng.*, vol. 8, no. 3, pp. 2455–2468, Jul. 2021.

[8] X. Wan, Y. Li, Y. Li, and M. Wu, "Finite-time H_∞ state estimation for two-time-scale complex networks under stochastic communication protocol," *IEEE Trans. Neural Netw. Learn. Syst.*, vol. 33, no. 1, pp. 25–36, Jan. 2022.

[9] C. Jia, J. Hu, D. Chen, Z. Cao, J. Huang, and H. Tan, "Adaptive event-triggered state estimation for a class of stochastic complex networks subject to coding-decoding schemes and missing measurements," *Neurocomputing*, vol. 494, pp. 297–307, Jul. 2022.

[10] X. Wan, Z. Wang, M. Wu, and X. Liu, "H_∞ state estimation for discrete-time nonlinear singularly perturbed complex networks under the round-robin protocol," *IEEE Trans. Neural Netw. Learn. Syst.*, vol. 30, no. 2, pp. 415–426, Feb. 2019.

[11] L. Wang, S. Liu, Y. Zhang, D. Ding, and X. Yi, "Non-fragile l_2-l_∞ state estimation for time-delayed artificial neural networks: An adaptive event-triggered approach," *Int. J. Syst. Sci.*, vol. 53, no. 10, pp. 2247–2259, Jul. 2022.

[12] Y. Liu, Z. Wang, and D. Zhou, "Scalable distributed filtering for a class of discrete-time complex networks over time-varying topology," *IEEE Trans. Neural Netw. Learn. Syst.*, vol. 31, no. 8, pp. 2930–2941, Aug. 2020.

[13] Z. Zhao, Z. Wang, L. Zou, Y. Chen, and W. Sheng, "Event-triggered set-membership state estimation for complex networks: A zonotopes-based method," *IEEE Trans. Netw. Sci. Eng.*, vol. 9, no. 3, pp. 1175–1186, May 2022.

[14] Y. Sun, X. Tian, and G. Wei, "Finite-time distributed resilient state estimation subject to hybrid cyber-attacks: A new dynamic event-triggered case," *Int. J. Syst. Sci.*, vol. 53, no. 13, pp. 2832–2844, Oct. 2022.

[15] J. Hu, Z. Wang, G.-P. Liu, and H. Zhang, "Variance-constrained recursive state estimation for time-varying complex networks with quantized measurements and uncertain inner coupling," *IEEE Trans. Neural Netw. Learn. Syst.*, vol. 31, no. 6, pp. 1955–1967, Jun. 2020.

[16] H. Dong, N. Hou, Z. Wang, and W. Ren, "Variance-constrained state estimation for complex networks with randomly varying topologies," *IEEE Trans. Neural Netw. Learn. Syst.*, vol. 29, no. 7, pp. 2757–2768, Jul. 2018.

[17] X. Meng, Y. Chen, L. Ma, and H. Liu, "Protocol-based variance-constrained distributed secure filtering with measurement censoring," *Int. J. Syst. Sci.*, vol. 53, no. 15, pp. 3322–3338, Nov. 2022.

[18] H. Gao, Z. Li, X. Yu, and J. Qiu, "Hierarchical multiobjective heuristic for PCB assembly optimization in a beam-head surface mounter," *IEEE Trans. Cybern.*, vol. 52, no. 7, pp. 6911–6924, Jul. 2022.

[19] H. Dong, Z. Wang, D. W. C. Ho, and H. Gao, "Variance-constrained H_∞ filtering for a class of nonlinear time-varying systems with multiple missing measurements: The finite-horizon case," *IEEE Trans. Signal Process.*, vol. 58, no. 5, pp. 2534–2543, May 2010.

[20] J. Hu, Z. Wang, S. Liu, and H. Gao, "A variance-constrained approach to recursive state estimation for time-varying complex networks with missing measurements," *Automatica*, vol. 64, pp. 155–162, Feb. 2016.

[21] Y. Zhang, Z. Wang, and L. Ma, "Variance-constrained state estimation for networked multi-rate systems with measurement quantization and probabilistic sensor failures," *Int. J. Robust Nonlinear Control*, vol. 26, no. 16, pp. 3507–3523, Nov. 2016.

[22] H. Dong, Z. Wang, B. Shen, and D. Ding, "Variance-constrained H_∞ control for a class of nonlinear stochastic discrete time-varying systems: The event-triggered design," *Automatica*, vol. 72, pp. 28–36, Oct. 2016.

[23] H. Geng, Z. Wang, Y. Chen, X. Yi, and Y. Cheng, "Variance-constrained filtering fusion for nonlinear cyber-physical systems with the denial-of-service attacks and stochastic communication protocol," *IEEE/CAA J. Autom. Sinica*, vol. 9, no. 6, pp. 978–989, Jun. 2022.

[24] Y. Gao, J. Liu, Z. Wang, and L. Wu, "Interval type-2 FNN-based quantized tracking control for hypersonic flight vehicles with prescribed performance," *IEEE Trans. Syst., Man, Cybern., Syst.*, vol. 51, no. 3, pp. 1981–1993, Mar. 2021.

[25] F. Yao, Y. Ding, S. Hong, and S.-H. Yang, "A survey on evolved LoRa-based communication technologies for emerging Internet of Things applications," *Int. J. Netw. Dynam. Int.*, vol. 1, no. 1, pp. 4–19, 2022.

[26] X. Wang, Y. Sun, and D. Ding, "Adaptive dynamic programming for networked control systems under communication constraints: A survey of trends and techniques," *Int. J. Netw. Dyn. Intell.*, vol. 1, pp. 85–98, Dec. 2022.

[27] J. Yang, L. Ma, Y. Chen, and X. Yi, "L_2-L_∞ state estimation for continuous stochastic delayed neural networks via memory event-triggering strategy," *Int. J. Syst. Sci.*, vol. 53, no. 13, pp. 2742–2757, Oct. 2022.

[28] P. Shi, W. Sun, X. Yang, I. J. Rudas, and H. Gao, "Master-slave synchronous control of dual-drive gantry stage with cogging force compensation," *IEEE Trans. Syst., Man, Cybern., Syst.*, vol. 53, no. 1, pp. 216–225, Jan. 2023.

[29] L. Zou, Z. Wang, J. Hu, and D. Zhou, "Moving horizon estimation with unknown inputs under dynamic quantization effects," *IEEE Trans. Autom. Control*, vol. 65, no. 12, pp. 5368–5375, Dec. 2020.

[30] M. B. Ignagni, "Separate bias Kalman estimator with bias state noise," *IEEE Trans. Autom. Control*, vol. 35, no. 3, pp. 338–341, Mar. 1990.

[31] X. Liu, "Design of delay-dependent state estimation algorithm for nonlinear coupling complex networks with dynamical bias: An adaptive event-triggered scheme," *Neurocomputing*, vol. 517, pp. 10–19, Jan. 2023.

[32] D. Liu, Z. Wang, Y. Liu, C. Xue, and F. E. Alsaadi, "Distributed recursive filtering for time-varying systems with dynamic bias over sensor networks: Tackling packet disorders," *Appl. Math. Comput.*, vol. 440, Mar. 2023, Art. no. 127669.

[33] W. Chen, Z. Wang, J. Hu, H. Dong, and G.-P. Liu, "Distributed resilient state estimation for cyber-physical systems against bit errors: A zonotopic set-membership approach," *IEEE Trans. Netw. Sci. Eng.*, vol. 10, no. 6, pp. 3922–3932, Nov./Dec. 2023, doi: 10.1109/TNSE.2023.3276851.

[34] W. Chen, Z. Wang, D. Ding, and H. Dong, "Consensusability of discrete-time multi-agent systems under binary encoding with bit errors," *Automatica*, vol. 133, Nov. 2021, Art. no. 109867.

[35] L. Wang, D. Zhao, Y. Zhang, D. Ding, and X. Yi, "Gain-scheduled state estimation for discrete-time complex networks under bit-rate constraints," *Neurocomputing*, vol. 488, pp. 120–129, Jun. 2022.

[36] P. Wen, X. Li, N. Hou, and S. Mu, "Distributed recursive fault estimation with binary encoding schemes over sensor networks," *Syst. Sci. Control Eng.*, vol. 10, no. 1, pp. 417–427, Dec. 2022.

[37] L. Zou, Z. Wang, B. Shen, H. Dong, and G. Lu, "Encrypted finite-horizon energy-to-peak state estimation for time-varying systems under eavesdropping attacks: Tackling secrecy capacity," *IEEE/CAA J. Autom. Sinica*, vol. 10, no. 4, pp. 985–996, Apr. 2023.

[38] L. Wang, D. Zhao, Y.-A. Wang, D. Ding, and H. Liu, "Partial-neurons-based state estimation for artificial neural networks under constrained bit rate: The finite-time case," *Neurocomputing*, vol. 488, pp. 144–153, Jun. 2022.

[39] Z. Liu, H. Gao, X. Yu, W. Lin, J. Qiu, J. J. Rodríguez-Andina, and D. Qu, "B-spline wavelet neural network-based adaptive control for linear motor-driven systems via a novel gradient descent algorithm," *IEEE Trans. Ind. Electron.*, vol. 71, no. 2, pp. 1896–1905, Feb. 2024.

[40] F. Yang, J. Li, H. Dong, and Y. Shen, "Proportional-integral-type estimator design for delayed recurrent neural networks under encoding–decoding mechanism," *Int. J. Syst. Sci.*, vol. 53, no. 13, pp. 2729–2741, Oct. 2022.

[41] H. Leung, C. Seneviratne, and M. Xu, "A novel statistical model for distributed estimation in wireless sensor networks," *IEEE Trans. Signal Process.*, vol. 63, no. 12, pp. 3154–3164, Jun. 2015.

[42] Q. Liu, Z. Wang, H. Dong, and C. Jiang, "Remote estimation for energy harvesting systems under multiplicative noises: A binary encoding scheme with probabilistic bit flips," *IEEE Trans. Autom. Control*, vol. 68, no. 1, pp. 343–354, Jan. 2023.

[43] Q. Liu and Z. Wang, "Moving-horizon estimation for linear dynamic networks with binary encoding schemes," *IEEE Trans. Autom. Control*, vol. 66, no. 4, pp. 1763–1770, Apr. 2021.

[44] N. Hou, Z. Wang, H. Dong, J. Hu, and X. Liu, "Sensor fault estimation for nonlinear complex networks with time delays under saturated innovations: A binary encoding scheme," *IEEE Trans. Netw. Sci. Eng.*, vol. 9, no. 6, pp. 4171–4183, Nov. 2022.

[45] P. Wen, H. Dong, F. Huo, J. Li, and X. Lu, "Observer-based PID control for actuator-saturated systems under binary encoding scheme," *Neurocomputing*, vol. 499, pp. 54–62, Aug. 2022.

[46] Z. Liu, W. Lin, X. Yu, J. J. Rodríguez-Andina, and H. Gao, "Approximation-free robust synchronization control for dual-linear-motors-driven systems with uncertainties and disturbances," *IEEE Trans. Ind. Electron.*, vol. 69, no. 10, pp. 10500–10509, Oct. 2022.

[47] B. Sereni, R. K. H. Galvão, E. Assunão, and M. C. M. Teixeira, "An output-feedback design approach for robust stabilization of linear systems with uncertain time-delayed dynamics in sensors and actuators," *IEEE Access*, vol. 11, pp. 20769–20785, 2023.

[48] Q. Zhang and Y. Zhou, "Recent advances in non-Gaussian stochastic systems control theory and its applications," *Int. J. Netw. Dynam. Int.*, vol. 1, no. 1, pp. 111–119, 2022.

[49] H. Chen, Z. Wang, B. Shen, and J. Liang, "Distributed recursive filtering over sensor networks with nonlogarithmic sensor resolution," *IEEE Trans. Autom. Control*, vol. 67, no. 10, pp. 5408–5415, Oct. 2022.

[50] C. Li, Z. Wang, W. Song, S. Zhao, J. Wang, and J. Shan, "Resilient unscented Kalman filtering fusion with dynamic event-triggered scheme: Applications to multiple unmanned aerial vehicles," *IEEE Trans. Control Syst. Technol.*, vol. 31, no. 1, pp. 370–381, Jan. 2023.

[51] Y. Gao, G. Sun, J. Liu, Y. Shi, and L. Wu, "State estimation and self-triggered control of CPSs against joint sensor and actuator attacks," *Automatica*, vol. 113, Mar. 2020, Art. no. 108687.

[52] W. Xu, G. Hu, D. W. C. Ho, and Z. Feng, "Distributed secure cooperative control under denial-of-service attacks from multiple adversaries," *IEEE Trans. Cybern.*, vol. 50, no. 8, pp. 3458–3467, Aug. 2020.

[53] C. Gao, X. He, H. Dong, H. Liu, and G. Lyu, "A survey on fault-tolerant consensus control of multi-agent systems: Trends, methodologies and prospects," *Int. J. Syst. Sci.*, vol. 53, no. 13, pp. 2800–2813, Oct. 2022.

[54] M. Cai, X. He, and D. Zhou, "Performance-improved finite-time fault-tolerant control for linear uncertain systems with intermittent faults: An overshoot suppression strategy," *Int. J. Syst. Sci.*, vol. 53, no. 16, pp. 3408–3425, Dec. 2022.

[55] M. Li, J. Liang, and F. Wang, "Robust set-membership filtering for two-dimensional systems with sensor saturation under the round-robin protocol," *Int. J. Syst. Sci.*, vol. 53, no. 13, pp. 2773–2785, Oct. 2022.

[56] D. Ding, Z. Wang, and Q.-L. Han, "A set-membership approach to event-triggered filtering for general nonlinear systems over sensor networks," *IEEE Trans. Autom. Control*, vol. 65, no. 4, pp. 1792–1799, Apr. 2020.

[57] J. Hu, C. Wang, R. Caballero-Águila, and H. Liu, "Distributed optimal fusion filtering for singular systems with random transmission delays and packet dropout compensations," *Commun. Nonlinear Sci. Numer. Simul.*, vol. 119, May 2023, Art. no. 107093.

[58] J. Hu, Z. Hu, R. Caballero-Águila, C. Chen, S. Fan, and X. Yi, "Distributed resilient fusion filtering for nonlinear systems with multiple missing measurements via dynamic event-triggered mechanism," *Inf. Sci.*, vol. 637, Aug. 2023, Art. no. 118950.

WEIJIAN LI received the B.Eng. degree in automation from Northeast Petroleum University, in 2021, where he is currently pursuing the master's degree in control engineering. His major research interests include complex networks and state estimation.

NAN HOU received the M.Eng. degree in control science and engineering and the Ph.D. degree in petroleum and natural gas engineering from Northeast Petroleum University, Daqing, China, in 2015 and 2018, respectively. In 2018, she was a Research Associate with the Department of Mathematics, City University of Hong Kong, Hong Kong, for three months. From 2019 to 2020, she was a Visiting Scholar with the Department of Computer Science, Brunel University London, London, U.K. She is currently an Associate Professor with the Artificial Intelligence Energy Research Institute, Northeast Petroleum University. Her current research interests include networked control systems, oil gas information, and control engineering.

FAN YANG received the M.Eng. degree in control science and engineering from Northeast Petroleum University, Daqing, China, in 2017. She is currently a Lecturer with the Artificial Intelligence Energy Research Institute, Northeast Petroleum University. Her current research interests include networked control systems, oil gas information, and control engineering.

XIANYE BU received the Ph.D. degree in petroleum and natural gas engineering from Northeast Petroleum University, Daqing, China. From 2018 to 2019, he was a Visiting Scholar with the Department of Computer Science, Brunel University London, London, U.K. He is currently an Associate Professor with the School of Electrical & Information Engineering, Northeast Petroleum University. His current research interests include networked control systems, oil gas information, and control engineering.

LIGANG SUN received the M.Eng. degree in control science and engineering from Northeast Petroleum University, in 2015. He is currently an Employee with CenerTech Tianjin Chemical Research and Design Institute Company Ltd.